



Simple and Complex Logical Functions in a SiC Tandem Device

Vitor Silva, Manuel A. Vieira, Paula Louro, Manuel Barata, Manuela Vieira

► To cite this version:

Vitor Silva, Manuel A. Vieira, Paula Louro, Manuel Barata, Manuela Vieira. Simple and Complex Logical Functions in a SiC Tandem Device. 5th Doctoral Conference on Computing, Electrical and Industrial Systems (DoCEIS), Apr 2014, Costa de Caparica, Portugal. pp.592-601, 10.1007/978-3-642-54734-8_66 . hal-01274828

HAL Id: hal-01274828

<https://inria.hal.science/hal-01274828>

Submitted on 16 Feb 2016

HAL is a multi-disciplinary open access archive for the deposit and dissemination of scientific research documents, whether they are published or not. The documents may come from teaching and research institutions in France or abroad, or from public or private research centers.

L'archive ouverte pluridisciplinaire **HAL**, est destinée au dépôt et à la diffusion de documents scientifiques de niveau recherche, publiés ou non, émanant des établissements d'enseignement et de recherche français ou étrangers, des laboratoires publics ou privés.



Distributed under a Creative Commons Attribution 4.0 International License

Simple and Complex Logical Functions in a SiC Tandem Device

V. Silva^{1,2}, M. A. Vieira^{1,2}, P. Louro^{1,2}, M. Barata^{1,2}, M. Vieira^{1,2,3}

¹Electronics Telecommunication and Computer Dept. ISEL, Lisboa, Portugal

²CTS-UNINOVA, Quinta da Torre, Monte da Caparica, 2829-516, Caparica, Portugal.

³DEE-FCT-UNL, Quinta da Torre, Monte da Caparica, 2829-516, Caparica, Portugal

Abstract. In this study we demonstrate the basic AND, OR and NOT logical functions based on SiC technology. The device consists of a p-i'(a-SiC:H)-n/p-i(a-Si:H)-n heterostructure with low conductivity doped layers. Experimental optoelectronic characterization of the fabricated device shows the feasibility of tailoring channel bandwidth and wavelength by optical bias through illumination at the back and front sides. Results show that, front background enhances the light-to-dark sensitivity of the long and medium wavelength range and strongly quenches the others. Back violet background has the opposite behavior; it enhances the magnitude in short wavelength range and reduces it in the long ones. This nonlinearity provides the possibility for selective removal or addition of wavelengths.

Keywords: Optoelectronics, Digital light signal, Logical functions, SiC Technology.

1 Introduction

Boolean algebra is the underlying mathematical theory that holds present computing systems. Since there is research to improve the materials that are used to build computational platforms there is also a need to guarantee that the basic logical functions are possible to be built and identified with such innovations.

Current CMOS technology is going to approach a scaling limitation in deep nanometer technologies. Quantum-dot cellular automata (QCA) is one of the promising new technologies for future generation ICs that overcome the limitation of CMOS. The fundamental unit of QCA-based design is majority gate; hence, efficient construction of QCA circuits using majority gates has attracted a lot of attention. Since every QCA circuit can be implemented by using only majority and inverter gates, the inverter becomes another important component in constructing QCA circuits [1].

Majority logic [2] is a way of implementing digital operations in a manner different from that of Boolean logic. The logic process of majority logic is more sophisticated than that of Boolean logic; consequently, majority logic is more powerful for implementing a

given digital function with a smaller number of logic gates. One of the most important component in any arithmetic and digital circuits in QCA and VLSI is the full adder [3], [4].

The majority gate can also be used for error correction in data transmission where several bits hold the pair functions of some selected bits (majority logic decoding) [5].

Research question answered in this article: Is it possible to use the SiC:H sensor for basic and complex logical functions?

Since previous work of the SiC:H sensor has proven its use as a multiplexer / demultiplexer device, and a multiplexer function allows for the construction of different logical functions, it is expected that by using this multiplexing capability that other logical functions can be identified with a SiC:H sensor.

2 Relationship to Collective Awareness Systems

A global earth picture of the present moment owes its possibility to a very remote past in which the global earth picture then would show reduced communities holding their bindings by being aware of everything that could endanger their survival or give them advantage over their everyday living. Communication is the basis for the collective awareness of a community. Collective awareness occurs when two or more people are aware of the same context and each is aware that the others are aware of it [6]. Visibility, awareness and accountability are properties of social translucent systems. To see is not to be aware, to be aware includes rules, some social, that govern our actions and through which we are responsible. For example, opening a door which has a sign "Please open slowly" does not force whoever opens it to do it with care, being aware that it may knock someone down. The person inside the room relies that the door will effectively be opened with care. This is a form of collective awareness. Privacy and visibility are different views, as it is for example a transparent door into a room. Collective awareness systems must be translucent. The action / interaction theory in sociology [7] is present when users interact with interfaces [8]. There is a cyclic action theory, in which the user acts by recognizing the effects that lead to his goal. Present society is covered with different objects that allow for collective awareness used for social sensing and social mining [9]. The sensor device that is presented in this manuscript allows for light sensing. Used as a social sensing device it may be used to distinguish colors [10], for people that have difficulty in this type of visualization. During daylight the sky color can be used as a collective sensing sensor and aid in weather forecasts. Used in social events, different lighting may become informative of special happenings and gather people's attention without using sound. Even though we can be aware of other people's constraints, this too is a collective awareness of constraints [6] that shape the way as we all participate in the process of organization.

3 Sensor Characterization and Operation

The sensor is a two stacked p-i-n structures (p(a-SiC:H)- i'(a-SiC:H)-n(a-SiC:H)-p(a-SiC:H)-i(a-Si:H)-n(a-Si:H)) sandwiched between two transparent contacts one at each end. The thicknesses and optical gap of the i' (200nm; 2.1 eV) and i- (1000nm; 1.8eV) layers are optimized for light absorption in the blue and red ranges [11]. Based in silicon carbon technology [12] this structure can be seen in Fig. 1, where the wavelength arrows indicate the absorption depths during operation and λ_V , λ_B , λ_G , λ_R the digital light signals within the visible spectrum.

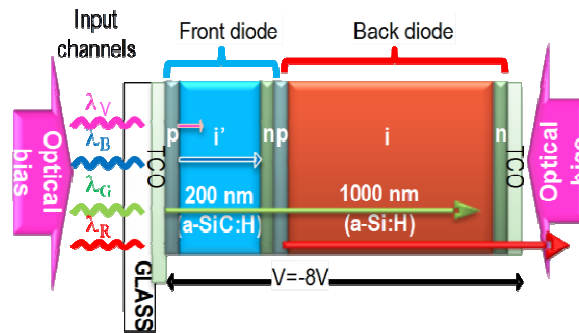


Fig. 1. Device structure and operation.

General purposes LEDs are used as light sources in two different ways: as digital signals and as background lighting. The digital signals are impinged on the front side of the sensor. The background lighting is either at the back or at the front side. The intensity of the signal sources is very low compared to the background intensity. Different wavelength signal sources are used: violet (400nm), blue (470nm), green (524nm) and red (626 nm). For background lighting the same violet wavelength is applied in a continuous and steady flux. When the background side changes the digital signals are sampled after transient influence has diminished.

The sensor is electrically biased with -8V. Readings were accomplished with a monochromator in 10nm steps from 400 to 800nm wavelengths.

Photocurrent results are presented in Fig. 2.

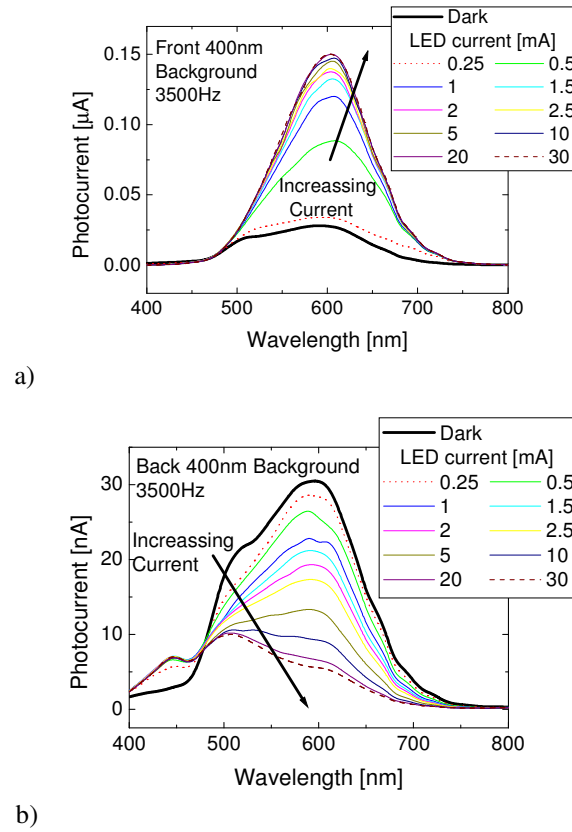


Fig. 2. Photocurrent with a) front and b) back lighting of the background.

The experimental results of Fig. 2a show the photocurrent's increase in the 470-700nm bandwidth. There is a significant increase just by the presence of the violet light; the fivefold increase from no LED current to 0.25mA is outstanding when compared to the increase from 0.25 to 30mA. In Fig. 2b the thick black curve is the same of the previous figure and represents the dark level. With increasing LED current the photocurrent in the 470-700nm bandwidth gradually decreases and there is an almost fixed increase of the photocurrent in the 400-470nm bandwidth. The photocurrent gain is the ratio between the photocurrent output and the value of the dark curve when there is no background lighting. This gain is shown in Fig. 3.

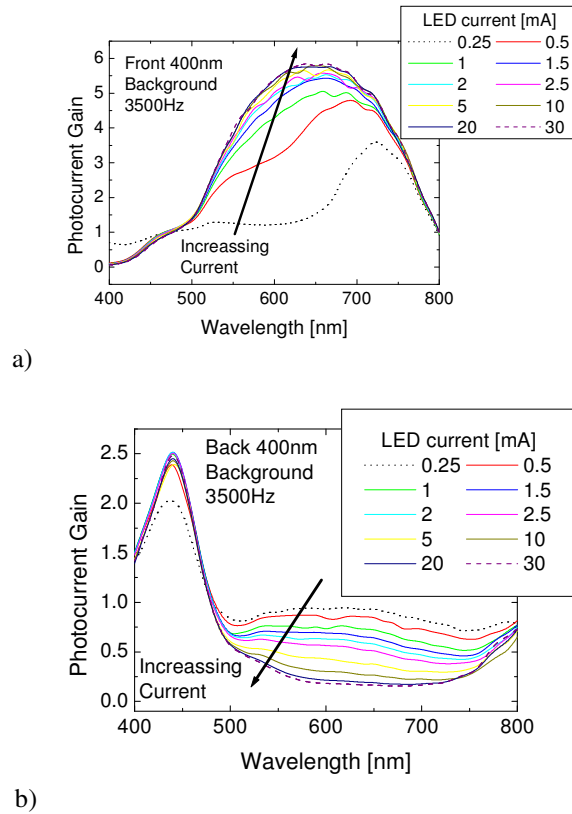


Fig. 3. Photocurrent gain when background light is at the a) front and b) back side of the device.

The spectral gain shown in Fig. 3a, with front background, reduces the short wavelengths ($<470\text{nm}$) and increases the long wavelengths ($>470\text{nm}$). This behavior is that of a selective filter centered in 650nm . The opposite happens when the background lighting is at the back side, Fig. 3b, the short wavelengths increase while the long wavelengths decrease. This is also a selective filter centered in 440nm . Thus the sensor can act as a selective filter, where the gain of the short and long pass wavelengths is controlled by optical bias at either one of the sides. The gains of both filters suffer almost no changes with LED currents above 10mA . These experimental results were made with the front Led positioned at 6.5cm from the sensor and the back LED at 2.5cm .

Normalizing the photocurrent gains shown in Fig. 3 and plotting them in the same graph, Fig. 4, enables a view of the two filters and the eye figure assures the effectiveness of the filtering capabilities of the sensor. A notch filter around 500nm is also perceived.

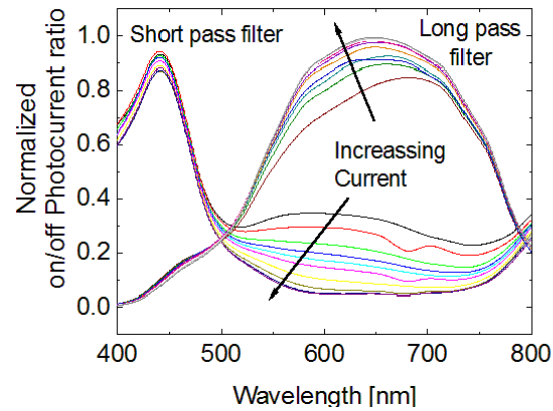


Fig. 4. Short and long pass filters.

The sensor biased at -8.00V and with no light shining in either of its surfaces presents a noise current which is depicted in Fig. 5 with a mean value of 0.89nA . The values were registered with a low-noise current preamplifier (SRS-SR570). Static power consumption is 7.15nW . The low values are due to the reverse polarization of the two pi^+npin junctions.

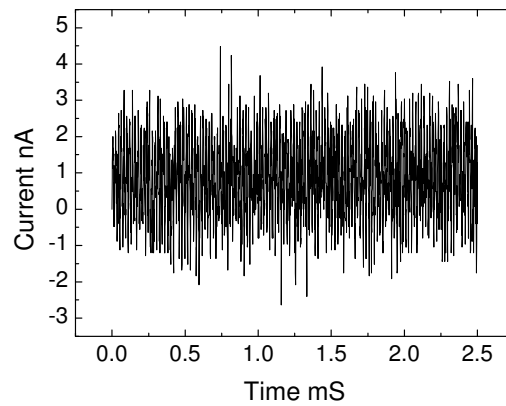


Fig. 5. Dark current.

4 Logical Functions

Logical functions are commonly used as logic gates [13] and by combining them, other logical functions are created, and some, due to their special function, are named. One of them is the multiplexer which is a combinational function. Due to its behavior the multiplexer can also be used as a basic circuit which in turn can produce results as simple as the basic logic gates. This functionality is presented in Fig. 6.

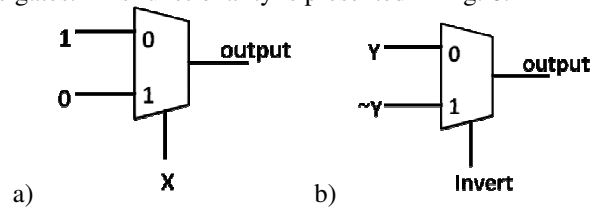


Fig. 6. A multiplexer used as an invert function.

The 2x1 multiplexer shown in Fig. 6a) is composed by a selector input, X, which chooses one of the input signals to be set as the output. When X hold the 0 value, the 0 input is set at the output, in this case the output presents the value 1. Accordingly, when X is 1 the output is 0. This means that the output is the inverse of X.

In Fig. 6b) the Invert signal is the selector that chooses between inputs Y and $\sim Y$ (NOT Y). The output follows the Y signal when the Invert selector is 0 and follows the $\sim Y$ signal when Invert is 1. By this setup, the Invert selector can choose between a Y signal or its inverse. This is the basis of the following work using the sensor's capability of being a multiplexer [14] to act as an inverter.

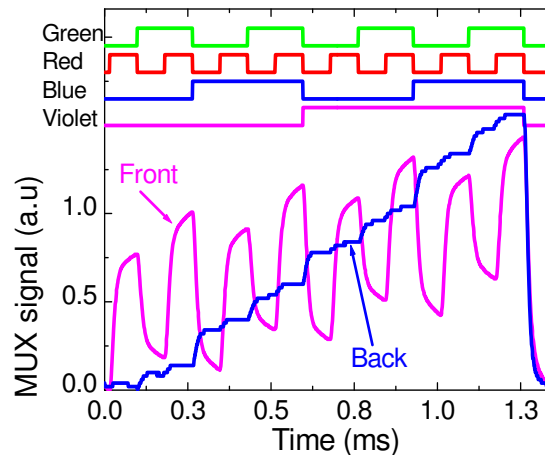


Fig. 7. The multiplex function.

Presented in Fig. 7 is the multiplex/demultiplex function of the SiC sensor. By choosing the front background the output signal follows the influence of the red and green digital light signals, and the back side lighting allows the output to follow the blue and violet signals. The patterns in the top of the figure are displayed to guide the eyes into the output signal. According to Fig. 4 the red and green wavelengths belong to the long wavelengths whereas the blue and violet wavelengths belong to the short wavelengths. Having in mind that choosing the background side chooses the wavelengths that are present at the output, and the behavior of the multiplexer in Fig. 6b it is possible to have a Y signal that belongs to the long wavelengths and a $\sim Y$ signal that belongs to the short wavelengths. This is presented in Fig. 8.

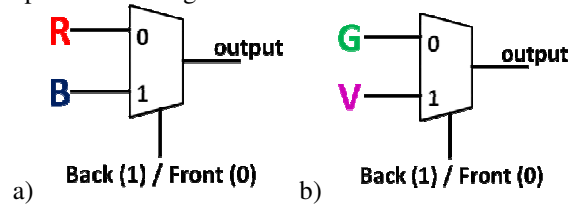


Fig. 8. Digital light multiplexer.

The digital light multiplexer presented in Fig. 8 works in the following way: the selector illuminates the background either at the front (0) or at the back (1), thus choosing a long wavelength (R or G) to be presented as output or the short wavelength (B or V). According to Fig. 6b, the R signal must have its inverse equal to $\sim B$, and the G signal its inverse equal to $\sim V$. The long, short wavelength pair forms a digital light signal and is represented by *Signal[Long, Short]*. In the experimental results that follow two different digital light signals will be used, signal D [Red, Blue] and signal P [Green, Violet].

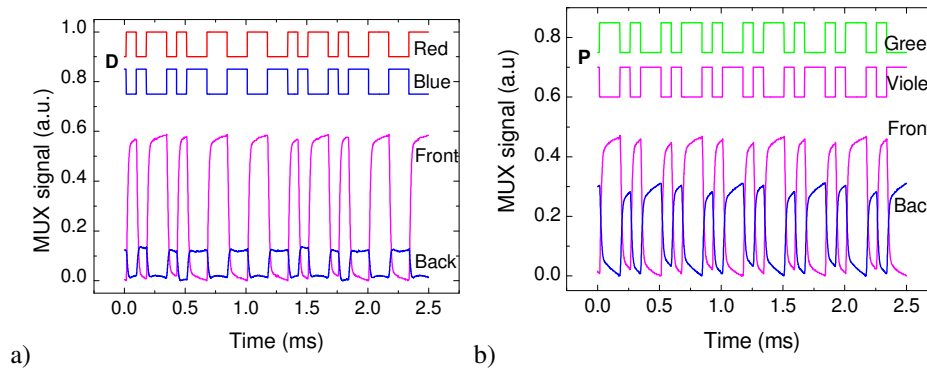


Fig. 9. Two digital light signals a) D [R, B] and b) P [G, V].

Plotted in Fig. 9a is the resultant output signal under front and back illumination for the same input digital light signal $D[R, B]$. The waveforms at the top of the figure represent the on/off input sequence. The front output follows the Red component of the digital signal and the back follows the Blue component. Fig. 9b is identical in its behavior, were the output signal with back lighting follows the Green component and the back waveform follows the Violet component. This shows the inverse function with two different examples. The simultaneous lighting of the digital signals D and P is presented in Fig. 10.

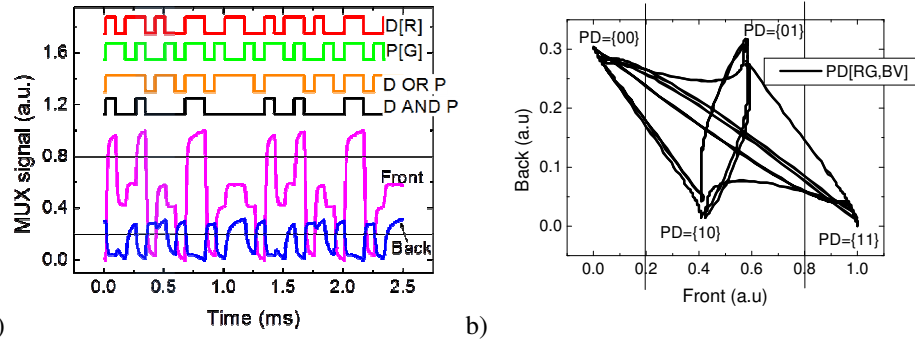


Fig. 10. a) Interaction of digital light signals D [R, B] and P [G, V]. b) Front and back signal correlation.

The two digital signals D and P applied simultaneously to the sensor are depicted in Fig. 10a. There are four different combinations. The shaded part in the figure holds these combinations that are shown with zoom in the next figures. The front and back signals can be plotted simultaneously showing the correlation between them in Fig. 10b. This allows the selection of threshold values that are used to determine the logical functions in Fig. 11 and Fig. 12. By adding a threshold line (not shown) at 0.15V on the back signal, all four combinations can be extracted. Noise will surround the vertexes of Fig. 10b creating areas of uncertainty which can be improved with hysteresis resulting in wider noise margins.

The waveforms at the top of Fig. 11a show the four different combinations of the digital signal D with P , only the long wavelength of each digital signal is shown. The output signal under front illumination is also depicted. By setting a threshold value above the minimum value of the output signal and assuming that values above the threshold have a logic value of 1 and the values below the line the logic value 0, the result is equal to the expected OR waveform. The sensor is thus capable of the OR logical function (disjunction).

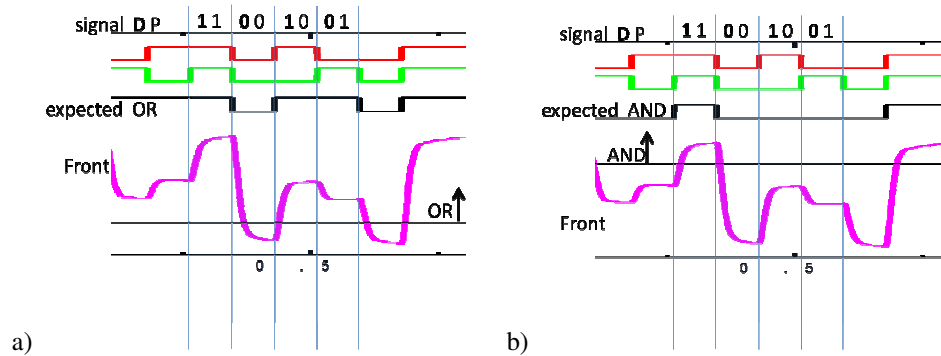


Fig. 11. a) The OR function. b) The AND function.

Depicted in Fig. 11b is the same figure of Fig. 11a, but with a different threshold line. The threshold line is slightly below the maximum value of the output signal under front background lighting. Values above the threshold line are considered as a logic value of 1, and those below the threshold line have logical value 0. Comparing this result with the expected AND waveform both coincide. The sensor is also capable of the AND logical function (conjunction).

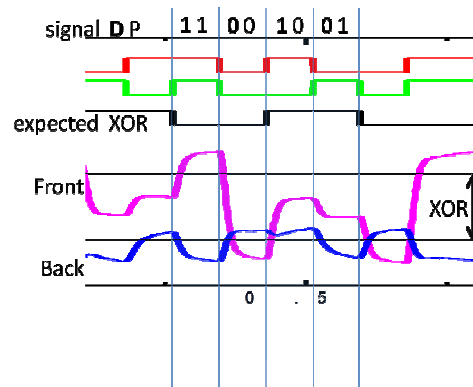


Fig. 12. The XOR function

The same description of Fig. 11a is applied to Fig. 12 which is completed with the threshold line of Fig. 11b and also displays the output under back illumination of the background. Using both threshold lines and setting the logic value 0 whenever the output signal under front illumination is below the minimum threshold and above the maximum threshold line, and setting the logic value 1 whenever the signal is in between the threshold lines, results in the equivalent values of the expected XOR waveform. The XOR function can also be identified by the following observation: comparing the output under

front with the output under back illumination, the expected XOR waveform has value 0 whenever front and back lines have derivatives with different sign and 1 when their signs are the same. This also equals the expected OR wavelength. The sensor is also capable of the XOR logical function (exclusive disjunction).

5 Conclusions

The SiC:H sensor has been studied as a multiplexor/demultiplexor device and with the possibility of determining the full 16 combinations of four digital inputs. The SiC:H sensor has the characteristic of a tunable filter in two distinct bandwidths, the long and short wavelengths. By defining a digital light signal as the combination of two wavelengths, one from the long and other from the short bandwidth it is possible to identify the inverse function using the tunable filter characteristic. The interaction of two digital light signals allow for the identification of other basic logical functions: AND, OR. The more complex digital function, the XOR is also a possible outcome of the sensor. The work that is under development aims for the identification of complex logical and arithmetic functions as the majority and the adder. The SiC:H sensor presented in this article is capable of logic functions and that is a good expectation that it can be used for optical computational systems.

References

1. M. R. Azghadi, O. Kavehei, and K. Navi, "A Novel Design for Quantum-dot Cellular Automata Cells and Full Adders," *J. Appl. Sci.*, vol. 7, no. 22, pp. 3460–3468, Dec. 2007
2. E. Pacuit and S. Salame, "Majority Logic Majority Logic : Syntax," pp. 598–605, 2004
3. R. Farazkish, S. Sayedsalehi, and K. Navi, "Novel Design for Quantum Dots Cellular Automata to Obtain Fault-Tolerant Majority Gate," *J. Nanotechnol.*, vol. 2012, pp. 1–7, 2012
4. M. R. Azghadi, O. Kavehei, and K. Navi, "A Novel Design for Quantum-dot Cellular Automata Cells and Full Adders," *J. Appl. Sci.*, vol. 7, no. 22, pp. 3460–3468, Dec. 2007
5. P. Hauck, M. Huber, J. Bertram, D. Brauchle, and S. Ziesche, "Efficient Majority-Logic Decoding of Short-Length Reed – Muller Codes at Information Positions," pp. 3–10
6. W. A. Kellogg and T. Erickson, "Social Translucence , Collective Awareness , and the Emergence of Place," pp. 1–6, 2002
7. C. Goodwin, "Action and embodiment within situated human interaction," *J. Pragmat.*, vol. 32, no. 10, pp. 1489–1522, Sep. 2000
8. H. Ryu and A. Monk, "Analysing interaction problems with cyclic interaction theory : Low-level interaction walkthrough," vol. 2, no. 3, pp. 304–330, 2004
9. F. Giannotti, D. Pedreschi, a. Pentland, P. Lukowicz, D. Kossmann, J. Crowley, and D. Helbing, "A planetary nervous system for social mining and collective awareness," *Eur. Phys. J. Spec. Top.*, vol. 214, no. 1, pp. 49–75, Dec. 2012
10. P. Louro, Y. Vygranenko, J. Martins, M. Fernandes, and M. Vieira, "Colour sensitive devices based on double p-i-n-i-p stacked photodiodes," vol. 515, pp. 7526–7529, 2007

11. M. Vieira, P. Louro, M. Fernandes, M. A. Vieira, Q. Torre, and M. Caparica, "Three Transducers Embedded into One Single SiC Photodetector : LSP Direct Image Sensor , Optical Amplifier and Demux Device," vol. March Ch19, pp. 403–426, 2011
12. G. De Cesare, F. Irrera, F. Lemmi, F. Palma, and M. Tucci, "a-Si:H/a-SiC:H Heterostructure for Bias-Controlled Photodetectors," MRS Proc., vol. 336, p. 885, Feb. 2011
13. W. Stallings, Computer Organization And Architecture Designing For Performance., 8th ed. Prentice Hall, pp. 694–730
14. M. Vieira, M. A. Vieira, V. Silva, P. Louro, and J. Costa, "SiC monolithically integrated wavelength selector with 4 channels," MRS Proc., vol. 1536, pp. 79–84, Jun. 2013